Response of steel fiber reinforced high strength concrete beams: Experiments and code predictions

Luigi Biolzi, Sara Cattaneo*
Department of Architecture, Built Environment and Construction Engineering (ABC), Politecnico di Milano, Piazza L. da Vinci, 33- 20133, Milan, Italy

The shear-flexure response of steel fiber reinforced concrete (SFRC) beams was investigated. Thirty-six reinforced concrete beams with and without conventional shear reinforcement (stirrups) were tested under a four-point bending configuration to study the effectiveness of steel fibers on shear and flexural strengths, failure mechanisms, crack control, and ductility. The major factors considered were compressive strength (normal strength and high strength concrete up to 100 MPa), shear span-effective depth ratio (a/d ¼ 1.5, 2.5, 3.5), and web reinforcement (none, stirrups and/or steel fibers).

The response of RC beams was evaluated based on the results of crack patterns, load at first cracking, ultimate shear capacity, and failure modes.

The experimental evidence showed that the addition of steel fibers improves the mechanical response, i.e., flexural and shear strengths and the ductility of the flexural members. Finally, the most recent code-based shear resistance predictions for SFRC beams were considered to discuss their reliability with respect to the experimental findings. The crack pattern predictions are also reviewed based on the major factors that affect the results.

Keywords: Steel fiber reinforced concrete, High-strength concrete, Shear strength, Shear span-depth ratio, Stirrups

1. Introduction

A promising solution for improving the mechanical performance of RC beams is to employ steel fiber-reinforced concrete [1,2]. It is well recognized that randomly distributed discontinuous steel fibers in a concrete matrix bridge tension cracks and enhance the overall response. In particular, experimental investigations have established that a suitable amount of steel fibers added to the concrete matrix significantly improves the shear and flexural strengths and ductility of steel fiber reinforced concrete (SFRC) flexural members [3,4]. As a consequence, fibers can potentially be used to replace conventional shear reinforcement, as shown in Refs. [5–13]. Despite the significant increase in concrete mix costs, the use of steel fiber reinforced concrete could be of interest to provide a design alternative for the shear reinforcement. Experimental investigations have been conducted to study the shear behavior of SFRC beams in the past [1,2,4–16]. In those papers, the effect of certain factors, such as shear span-effective depth ratio, fiber volume content, concrete strength, and longitudinal reinforcement ratio on the shear strength of SFRC members have been discussed. Although several experimental studies have been conducted to date to evaluate the shear capacity of SFRC beams, few studies are available on the shear strength of high strength SFRC members [14–16]. Hence, further experiments are needed to assess the response of high strength SFRC beams, especially with reference to more recent code provisions. Indeed, the influence of steel fibers in enhancing the shear strength of reinforced concrete (RC) members has been recognized in the fib Model Code for Concrete Structures 2010 (MC2010) and ACI 318 [17,18]. In the MC2010 [17], fiber reinforced concrete is considered as a material for structural members. The shear resistance of FRC members without shear reinforcement is defined as an extension of the shear strength suggested by Eurocode 2 [19]; an additional term that included the toughness properties of FRC is introduced by modifying the longitudinal reinforcement ratio. The ACI 318-11 Code allows a partial replacement of the minimum shear reinforcement with a fiber amount greater than 0.75% of the volume in the concrete composition (crimped or hooked fibers) for a concrete strength lower than 40 MPa and beam depth lower than 60 cm.

The prediction models to calculate the shear resistance (all of

Article history:
Received 9 August 2015
Received in revised form
28 November 2016
Accepted 7 December 2016
Available online 13 December 2016

* Corresponding author.
E-mail addresses: luigi.biolzi@polimi.it (L. Biolzi), sara.cattaneo@polimi.it (S. Cattaneo).

Published Journal Article available at: http://dx.doi.org/10.1016/j.cemconcomp.2016.12.002

them empirical) are unavoidably affected by the complexity of the problem. As stated above, the shear resistance is a function of several parameters such as shear span to effective depth ratio, longitudinal reinforcement ratio, fiber volume, fiber aspect ratio, and concrete tensile and compressive strengths.

As observed in Ref. [7], a first group of prediction models considers concrete and fibers with a separate contribution to shear resistance, whereas a second group suggests improved concrete shear resistance directly. A more coherent method, with a strain-based approach, has been suggested by Choi et al. [20].

This paper takes an experimental approach to study the shear-flexure response of steel fiber reinforced concrete beams. Thirty-six reinforced concrete beams, with and without conventional shear reinforcement (stirrups), were tested under a four-point bending configuration to investigate the effectiveness of steel fibers on shear and flexural strengths, failure mechanisms, crack control, and ductility.

Both normal vibrated concrete and high strength concrete beams (up to 100 MPa) were considered. Three different groups categorized by their shear span-effective depth ratio (a/d = 1.5, 2.5, 3.5) were tested. The response of reinforced concrete (RC) beams was assessed based on the results of crack patterns, load at first cracking, ultimate shear capacity, and failure modes. The experimental evidence confirmed that the addition of steel fibers improved the mechanical response, both in terms of flexural and shear strengths and the ductility of the flexural members. The most recent code-based shear resistance formulas for RC beams are considered; additionally, the crack pattern predictions are reviewed based on the major factors that affect the results.

2. Experimental research

The experimental program considered three types of concrete designed for a compressive strength f_{ck}, at 28 days, of approximately 40, 75 and 90 MPa. The mix-design and the main mechanical properties at the time of the test are reported in Table 1.

The compressive strength was evaluated on the 150 mm standard cube (at least three), the tensile strength on plain concrete was evaluated by splitting tests (diameter 100 mm length 200 mm), and the bending strength was evaluated on prisms (side 150 × 150 × 600 mm) on a three-point test configuration according to EN 14651 [21]. For fiber reinforced concretes, the associated stress at a Crack Mouth Opening Displacement (CMOD) of 0.5 mm (f_{R1}) and of 2.5 mm (f_{R3}) are also reported (Fig. 1).

The high strength concretes were made with the addition of different mineral admixtures: fly ash was added to the concrete

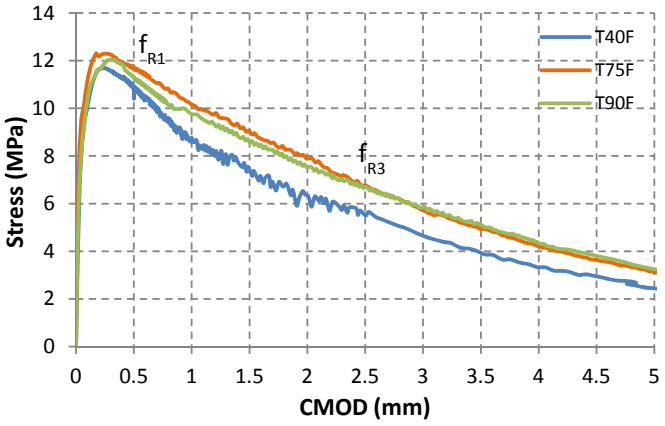

Fig. 1. Bending test on concrete T75F: CMOD vs stress.

with the characteristic strength of 75 MPa, while microsilica was added to the mix with the strength of 90 MPa. For each type of concrete, two mixes were considered, plain and with steel hooked fibers of low (40) and high tenor (75 and 90) carbon content, and length of 30 mm. The first type of fibers had an aspect ratio equal to 48 and a tensile strength of 1250 MPa, while the second type had an aspect ratio equal to 79 and a tensile strength of 2300 MPa. The powder addition (microsilica and fly ash) led to a different compressive strength at the time of the test with respect to the designed one.

Beams of three different span/depth ratios were cast (Fig. 2):

- S: 15 × 30 × 240 cm^3 tested with shear span a/d = 1.5;
- M: 15 × 30 × 290 cm^3 tested with shear span a/d = 2.5;
- L:15 × 30 × 340 cm^3 tested with shear span a/d = 3.5.

For each size and mix, beams with and without stirrups (diameter ϕ 6/15 cm) were examined, a total of 36 beams. All specimens had the same longitudinal reinforcement B450C (2 ϕ 16), while in the beams with shear reinforcement, 2 ϕ 8 were used as compression steel. The average yielding strength of the longitudinal reinforcement was 522 MPa and that of transversal reinforcement was 533 MPa. The effective depth of the cross section, d, was 26 cm.

Each beam was given a proper code in order to identify all the features: T-$f_{ck,cube}$ (compressive strength)- size (S, M or L) -shear reinforcement (N = none, S = stirrups)- fibers (N = none, F = fibers).

Table 1
Mix-design and mechanical characteristics.

	T40	T40F	T75	T75F	T90	T90F
Cement CEM II-AL 42,5 R (kg/m^3)	300	300	//	//	//	//
Cement CEM I 52,5 R (kg/m^3)	//	//	380	380	405	405
Fly ash (kg/m^3)	80	80	60	60	//	//
Microsilica in slurry al 50% (kg/m^3)	//	//	//	//	90	90
Sand + aggregates (kg/m^3)	1870	1870	1905	1905	1920	1920
Naphthalene sulfonate superplasticizer (l/m^3)	4.5	6	//	//	//	//
Acrylic superplasticizer (l/m^3)	//	//	5,5	7	10	12
Water (l/m^3)	175	175	150	150	80	80
Steel fiber low tenor C (kg/m^3)	//	50	//	//	//	//
Steel fiber high tenor C (kg/m^3)	//	//	//	50	//	70
f_{cm} (MPa)	64.5	62.5	86.7	104.8	94.9	91.8
Standard Deviation (MPa)	4.7	4.4	9.8	0.6	7.7	7.3
f_{ctm} (MPa)	4.6		5.1		5.3	
f_{cfm} (MPa)	6.85	11.70	8.03	12.30	7.41	12.04
f_{R1} (MPa)		10.40		11.70		11.26
f_{R3} (MPa)		5.50		6.76		6.7

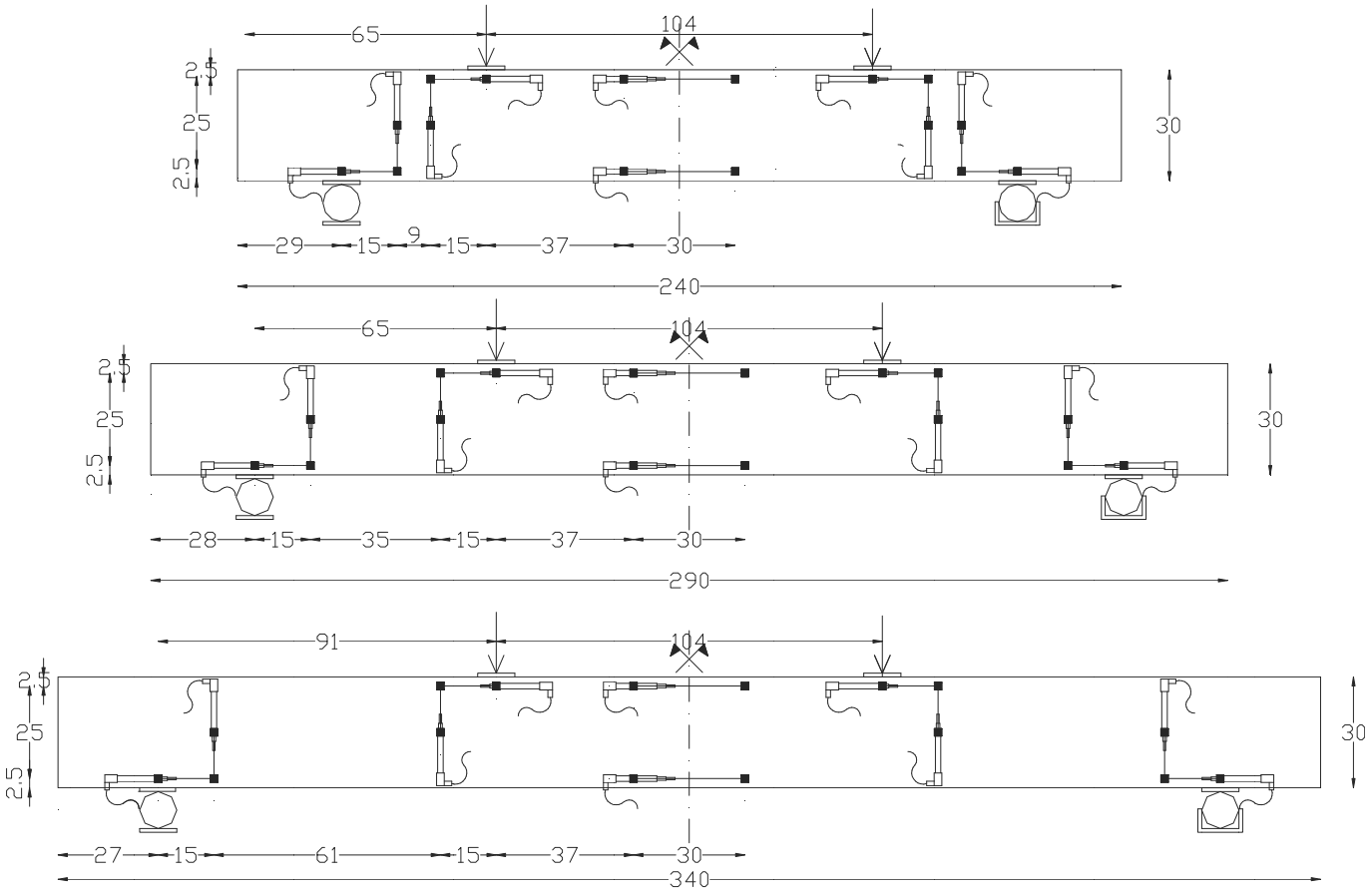

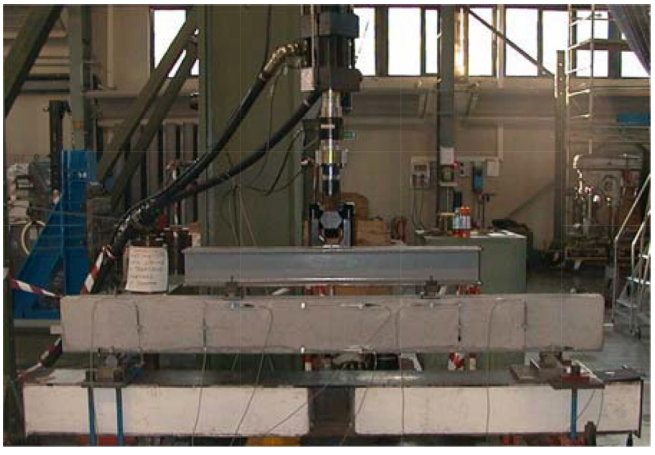

Fig. 2. Test configuration (measure in cm).

The tests on medium and long beams were carried out with an MTS hydraulic jack with a load capability of 250 kN, while for the short specimens, another MTS hydraulic jack of 1000 kN was used. The tests were displacement controlled, and the beams were monitored by means of 10 inductive transducers (LVDT± 5 mm) set as shown in Fig. 2. A potentiometer, 25 cm gage length, was placed on the middle section to measure the vertical displacement.

3. Experimental results

Different behavior and failure modes were observed depending on the shear reinforcement, fibers and shear span-to-depth ratio. Fig. 3 shows typical crack patterns for each type of reinforcement.

In all cases during the test, cracks appeared between the load points (constant bending moment). By increasing the load, other cracks appeared in the regions with shear and flexure, leading to beam failure.

In particular, beams without fibers and without stirrups (NN) exhibited a brittle diagonal shear failure as shown in Fig. 3, for shear span-to-depth ratios of 2.5 and 3.5. Short beams presented the same type of shear failure, but the overall response showed ductility (Fig. 5).

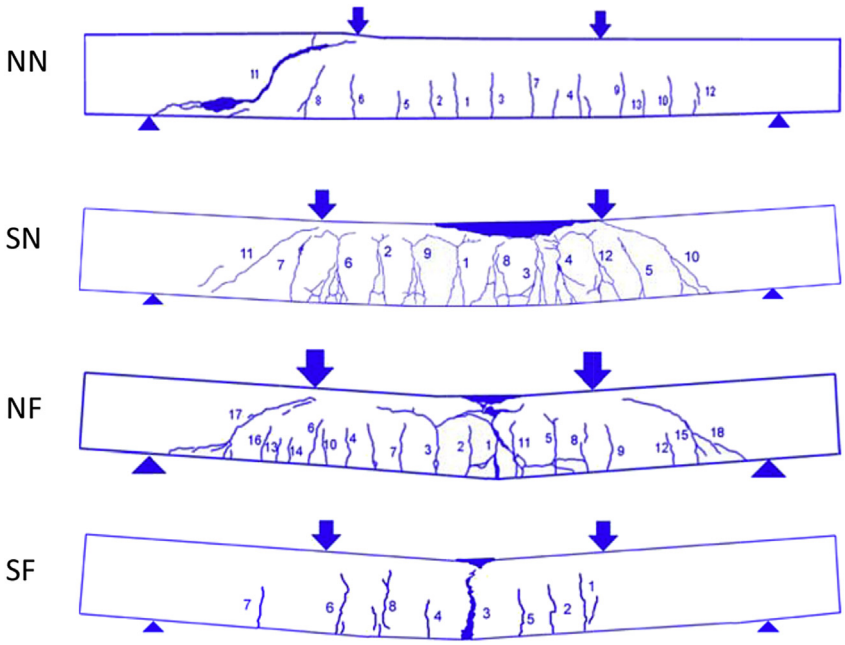

Fig. 3. Typical crack patterns.

Beams with stirrups as shear reinforcement (SN) were characterized by a more ductile behavior (Fig. 5). Concrete crushing in the compressive zone (Fig. 3) and a large number of cracks with branching led to failure with the detachment of a large material volume.

Beams with fibers, both with (SF) and without stirrups (NF), failed in a ductile manner by flexure (Fig. 5).

Also in these cases, a large number of cracks were observed, with the main crack leading to beam failure with the rupture of the longitudinal rebar and crushing of the concrete in the compressive zone of the beam (Fig. 3).

For the amount of fibers considered, it appears that shear reinforcement did not influence the type of failure.

4. Discussion

In Table 2, the maximum moment and the type of failure are reported. It may be observed that with the exception of beams without fiber and without stirrups, all beams made with the same mix and reinforcement exhibit the same type of failure and similar maximum moment. Short beams without fibers and without shear reinforcement collapsed by diagonal failure but with significant ductility, whereas longer beams failed in brittle manner due to diagonal failure (in one case, the diagonal failure was followed by bond collapse).

Fig. 4 shows the maximum moments obtained for the different type of beams, with fiber-reinforced concrete leading the way. In fact, it seems that for the geometries and the fiber amount considered, stirrups do not alter the type of failure and the maximum moment. Obviously, without fibers, stirrups have a fundamental influence, except in the case of short beams, where the small shear span—to-depth ratio (1.5) led to a ductile post peak branch due to the arch action.

The considered parameters (compressive strength, fibers, shear reinforcement, shear span to depth ratio) also had a fundamental influence on the moment-displacement curves as shown in the following.

4.1. Influence of fibers and shear reinforcement

Fibers and shear reinforcement affect not only the ultimate load but also the overall structural behavior. Fig. 5 shows the moment-displacement curves for small, medium, and long beams with the same compressive strength (T90), comparing different reinforcements.

Up to cracking (bending moment between 12 and 15 kNm), the

Table 2
Maximum moment and type of failure: D (diagonal shear failure) – B (bond failure) - F (flexure) – C (compressive zone crushing).

Beam	M_{max}(kNm)	Failure	Beam	M_{max}(kNm)	Failure	Beam	M_{max}(kNm)	Failure
Short			Medium			Long		
T40S-NN	50,90	D	T40M-NN	35,95	D+B	T40L-NN	37,87	D
T40S-SN	53,29	C	T40M-SN	51,47	C	T40L-SN	51,25	C
T40S-NF	56,21	F	T40M-NF	55,42	F	T40L-NF	54,69	F
T40S-SF	54,85	F	T40M-SF	54,46	F	T40L-SF	53,76	F
T75S-NN	51,78	D	T75M-NN	48,33	D+C	T75L-NN	49,96	D
T75S-SN	53,33	C	T75M-SN	54,38	C	T75L-SN	53,56	C
T75S-NF	64,37	F	T75M-NF	62,25	F	T75L-NF	62,07	F
T75S-SF	63,90	F	T75M-SF	62,88	F	T75L-SF	63,82	F
T90S-NN	54,93	D	T90M-NN	33,71	D	T90L-NN	43,52	D
T90S-SN	52,31	C	T90M-SN	52,45	C	T90L-SN	52,58	C
T90S-NF	62,77	F	T90M-NF	64,75	F	T90L-NF	63,91	F
T90S-SF	62,76	F	T90M-SF	62,75	F	T90L-SF	62,05	F

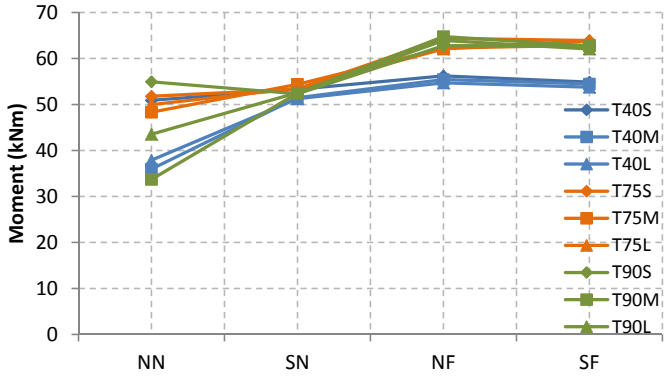

Fig. 4. Maximum moments.

behavior of all beams was similar, while in the inelastic range, fibers (both with and without stirrups) enhanced strength, ductility, and stiffness in all cases. As stated above, it appears that in fiber reinforced beams, stirrups did not modify the overall behavior, as shown by the similar curves (Fig. 5 - NF, SF). Comparing beams without conventional reinforcement, with and without fibers (NN, NF), it may be observed that fibers strongly affect the results, not only in terms of strength, but above all in terms of ductility. In fact, except for short beams, the failure of unreinforced beams was due to brittleness. Short beams without fibers exhibited a similar response both with and without stirrups (NN, SN).

Because fiber-reinforced beams did not exhibit shear failure, it could be interesting to check whether the sectional analysis for SFRC proposed by MC2010 [17] is able to predict the ultimate state limit design moment. This moment is calculated considering a rectangular stress distribution for concrete both in tension and in compression (Fig. 6). The proposed analysis takes into account both the effect of fibers and of high strength concrete. The latter is calculated considering two factors, λ (which defines the height of the compressive zone) and η (which defines the effective strength), as follows:

$$\lambda = 0.8 \quad \text{for} \quad f_{ck} \leq 50\text{MPa}$$

$$\lambda = 0.8 - (f_{ck} - 50)/400 \quad \text{for} \quad 50 \leq f_{ck} \leq 100\text{MPa}$$

and

$$\eta = 1 \quad \text{for} \quad f_{ck} \leq 50\ \text{MPa}$$

$$\eta = 1 - (f_{ck} - 50)/200 \quad \text{for} \quad 50 < f_{ck} \leq 100\ \text{MPa}$$

The contribution of steel fibers is established assuming a uniform stress distribution equal to f_{Ftdu} and evaluated according to MC2010 [17] (section 5.6) on the basis of the experimental results from bending tests (based on EN14651 [21]) (Table 1).

Table 3 reports the average experimental maximum moment and its coefficient of variation (v) for each beam type (Type NN is not considered as those beams exhibited shear failure), the ultimate limit moment (M_{Rd}) assessed considering the design value of the materials' properties, and the ratio between the experimental and the design bending moment. This last parameter, which could be considered as a safety factor, varies between 1.27 and 1.41. For beams made of concrete T75F and T90F, the safety factor is similar to that of beams without fiber steel reinforcement, whereas concrete T40F shows a lower safety factor. Nevertheless, it seems that MC2010 [17] is a suitable design code even for fiber-reinforced concrete. This is confirmed by considering the ratio between the experimental and the "theoretical" (M_{th}) moments evaluated according to MC2010 [17], considering the actual materials' properties (average experimental strengths of concrete and reinforcement) without (M_{th*}) or with (M_{th**}) the contribution of steel fibers (Table 3).

Note that for concrete without steel fibers, the prediction of MC2010 [17] is excellent, while it seems that neglecting the tensile strength, the ultimate moment is underestimated approximately 20% for beams T75 and T90 and between 4 and 7% for beam T40, respectively.

The fiber contribution was accounted for considering the design tensile strength f_{ctd}, determined with the stress f_{R3} associated at the value of the CMOD equal to 2.5 mm according to MC2010.

The resulting theoretical moment M_{th**} underestimates the experimental moment of T75 and T90 by approximately 6% and overestimates the experimental moment of T40 by approximately 5%. Indeed, by considering a rigid plastic stress distribution (Fig. 6), a proper value of the tensile strength should be chosen according to the actual stress-strain curve, and assuming a single value at a certain displacement seems too simplistic.

Nevertheless, it is worth noting that for design reasons, MC2010 [17] seems to be an excellent guideline, since the safety factor is similar for both plain and SFRC.

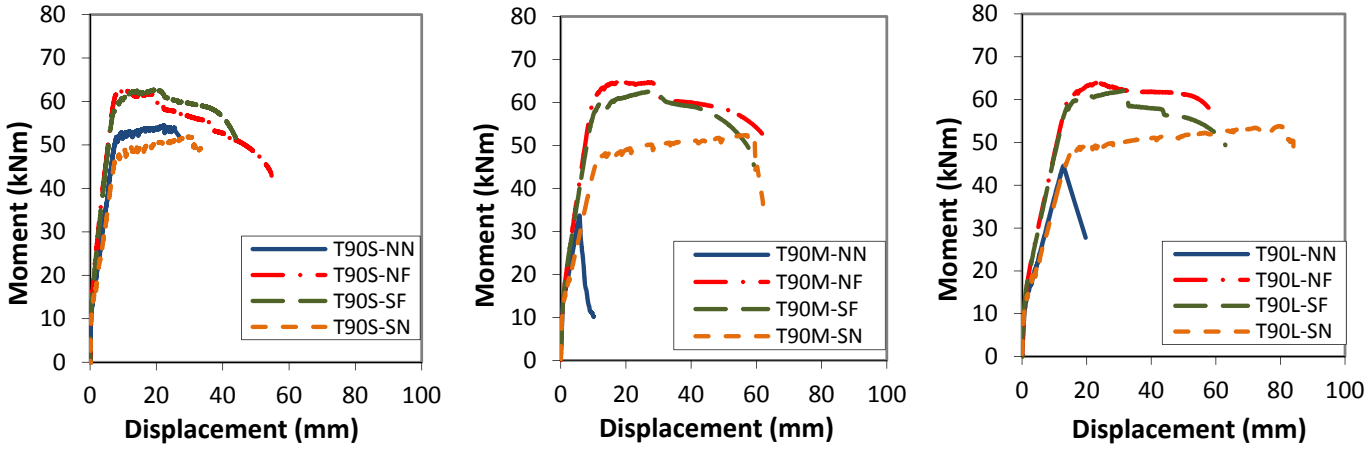

Fig. 5. Moment-displacement curves: Influence of fibers and shear reinforcement.

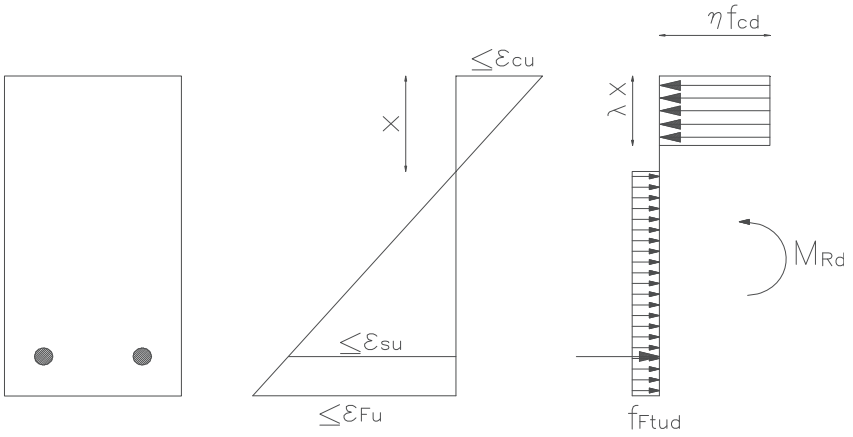

Fig. 6. ULS for bending moment - Simplified stress-strain relationship according to MC2010 [17].

Table 3
Average experimental moment, design moment, ratios between experimental and predicted moments.

Beam Type	Average M_{max} (kNm)	v (%)	M_{Rd} (kNm)	M_{max}/M_{Rd}	M_{max}/M_{th}^{*}	M_{max}/M_{th}^{**}
T40-SN	52.00	2.15%	37.98	1.37	1.00	
T40-NF	55.44	1.37%	42.74	1.30	1.07	0.96
T40-SF	54.36	1.02%	42.95	1.27	1.04	0.94
T75-SN	53.76	1.03%	38.16	1.41	1.02	
T75-NF	62.90	2.03%	45.55	1.38	1.20	1.05
T75-SF	63.53	0.89%	45.49	1.40	1.20	1.06
T90-SN	52.45	0.26%	38.28	1.37	0.99	
T90-NF	63.81	1.56%	45.12	1.41	1.22	1.07
T90-SF	62.52	0.65%	45.1	1.39	1.18	1.05

4.2. Influence of the concrete compressive strength

Beams made with different concrete grades, without fibers and with stirrups but with the same reinforcement and shear span-to-depth ratio, showed a similar overall response (Fig. 7). In all other cases, however, the strength and the stiffness increased with the concrete grade. Note that the curves T75 and T90 are similar because at the time of the test, the average compressive strengths were comparable.

To discuss the behavior of the different types of beams and to take into account the different concrete strengths (f_{cm}), it is useful to evaluate the normalized shear strength as:

$$\tau_{nn} = \frac{V_{max}}{bd\sqrt{f_{cm}}} \quad (1)$$

Fig. 8 shows the normalized shear strength as a function of the shear span to depth ratio of beams without stirrups – with/without fibers (a), with stirrups – with/without fibers (b), without fibers – with/without stirrups (c), with fibers – with/without stirrups (d).

In all cases, it seems that high strength concrete presented a lower performance with respect to normal strength concrete. Indeed, even if the higher strength was achieved with concrete C90, the higher normalized shear strength was always reached with concrete C40. This experimental evidence could be explained by the higher bond strength between the fiber and the concrete matrix in the higher strength concrete, leading to the fracture of some fibers (instead of fiber pullout across cracks).

In addition, the limited aggregate interlock in high strength concrete could be a parameter that affected the results. In this concrete, the higher strength of the concrete matrix and interfacial transition zone lead to the fracture of the aggregates, as shown in Fig. 9, resulting in a limited interlock. Indeed, in all high-performance beams, the observed fracture passed across the aggregates.

On the other hand, it is clear that fibers have a strong effect in beams without stirrups and improve the response in beams with stirrups. The comparison between beams with fibers with/without stirrups (Fig. 8d) shows that fibers are more effective than stirrups. Clearly, this is valid for the type and amount of fibers considered.

The influence of the different concrete strength seems to be reduced when the beam length is increased.

4.3. Influence of shear span to depth ratio

Table 2 and Fig. 4 show that in beams with a web reinforcement (stirrups and/or fibers) that failed in flexure, the shear span-to-depth ratio did not affect the response. Conversely, in the case of beams without fibers and without stirrups, this parameter had a strong influence on the experimental results. Fig. 10 shows the maximum moment as a function of the shear span-to-depth ratio. For all concrete grades, the lower moment was obtained for the shear span-to-depth ratio of 2.5, while short beams (a/d = 1.5) led always to a higher moment due to the arch action. The results obtained for beams T40 and T90 agree with the typical Kani's valley [22], while beam T75M-NN showed an atypical behavior.

In this case, the shear failure produced a limited crushing of the compression chord (Fig. 11a). This second type of failure emerged after the first sudden drop (indicated with the arrow in Fig. 11b) in the moment displacement curve. The displacement control setup of the test helped to avoid the brittle shear collapse and the development of another failure mechanism, which involved a concrete crushing in the compression chord. Short beams always led to a higher moment due to the arch action.

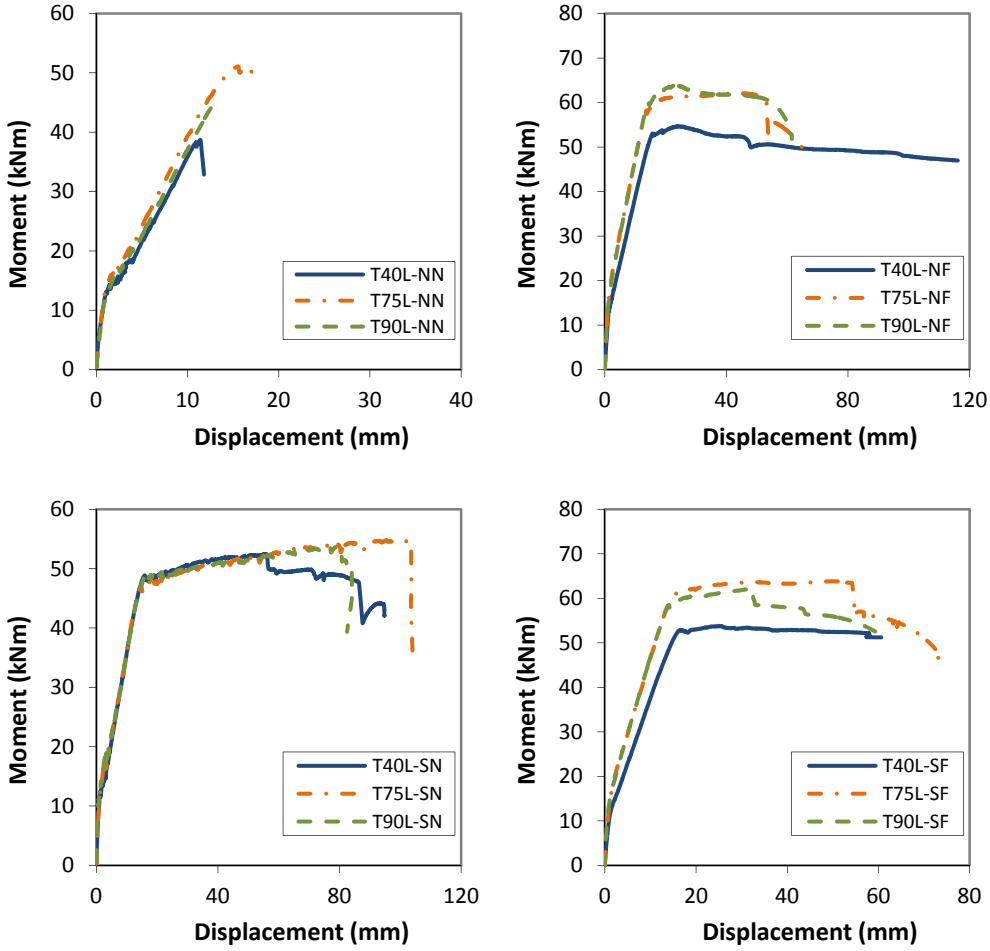

Fig. 7. Moment-displacement curves: Influence of concrete strength.

4.4. Cracking behavior

The experimental evidence showed different crack onsets and crack patterns depending on the concrete and beam type.

Table 4 reports the average experimental and theoretical cracking moment ($M_{cr,exp}$, $M_{cr,th}$), crack opening (w_{exp}, w_{th}), and spacing (s_{exp}, s_{th}).

It appears that fibers increased the experimental cracking moment by approximately 20% only for concretes T75F and T90F. For other concrete mixes, the cracking moment was quite similar (coefficient of variation of approximately 8%). Stirrups seem to have a minor effect on the cracking moment (which was slightly lower in beams with shear reinforcement), while they strongly affected the crack-opening in beams without fibers. Indeed, for the SFRC, the crack opening and the crack spacing were smaller with respect to the counterpart without fibers. In beams without stirrups and fibers, however, the crack openings were larger (increase of crack opening of approximately 27% with respect to beams with stirrups). The main parameter that affects the crack spacing seems to be fiber reinforcement, which leads to a reduction of approximately 28%.

The experimental cracking moment was visually detected and confirmed by the load-displacement curve, while its theoretical value was evaluated as:

$$M_{cr,th} = \left(f_{ctm,fl} - \sigma_{sh}\right) W^*_{\text{inf}} \tag{2}$$

where $W^*_{\text{inf}} = I^*/y_{\text{inf}}$ is the section modulus of the homogenized section, $f_{ctm,fl}$ is the flexural tensile strength, and σ_{sh} is the stress in the concrete due to shrinkage. The flexural tensile strength and the strain due to shrinkage were evaluated according to MC2010 [17] on the basis of the compressive strength for both plain and fiber-reinforced concrete.

Fig. 12 shows the ratio between the experimental cracking moment and the theoretical one. Note that there is good agreement between the experimental and theoretical results for fiber reinforced beams, while the prediction for beams without fibers and with shear reinforcement does not appear to be accurate. The prediction for beams without shear reinforcement (with or without fibers) is very good, with the exception of concrete T90. In this case, however, the experimental cracking moment was much lower (lower than the one observed in concrete T40).

The experimental crack opening and crack spacing (Table 4) were assessed at a load level associated with the design moment (approximately 38 kNm for plain concrete and 45 kNm for fiber reinforced concrete) and taking into account flexural cracks only (in the central region of the beam under a constant bending moment).

The design moment of fiber reinforced concrete was evaluated according to MC2010 [17], considering the simplified stress distribution (rigid-plastic) for concrete in tension.

According to code, the theoretical crack width w_{th} can be evaluated as:

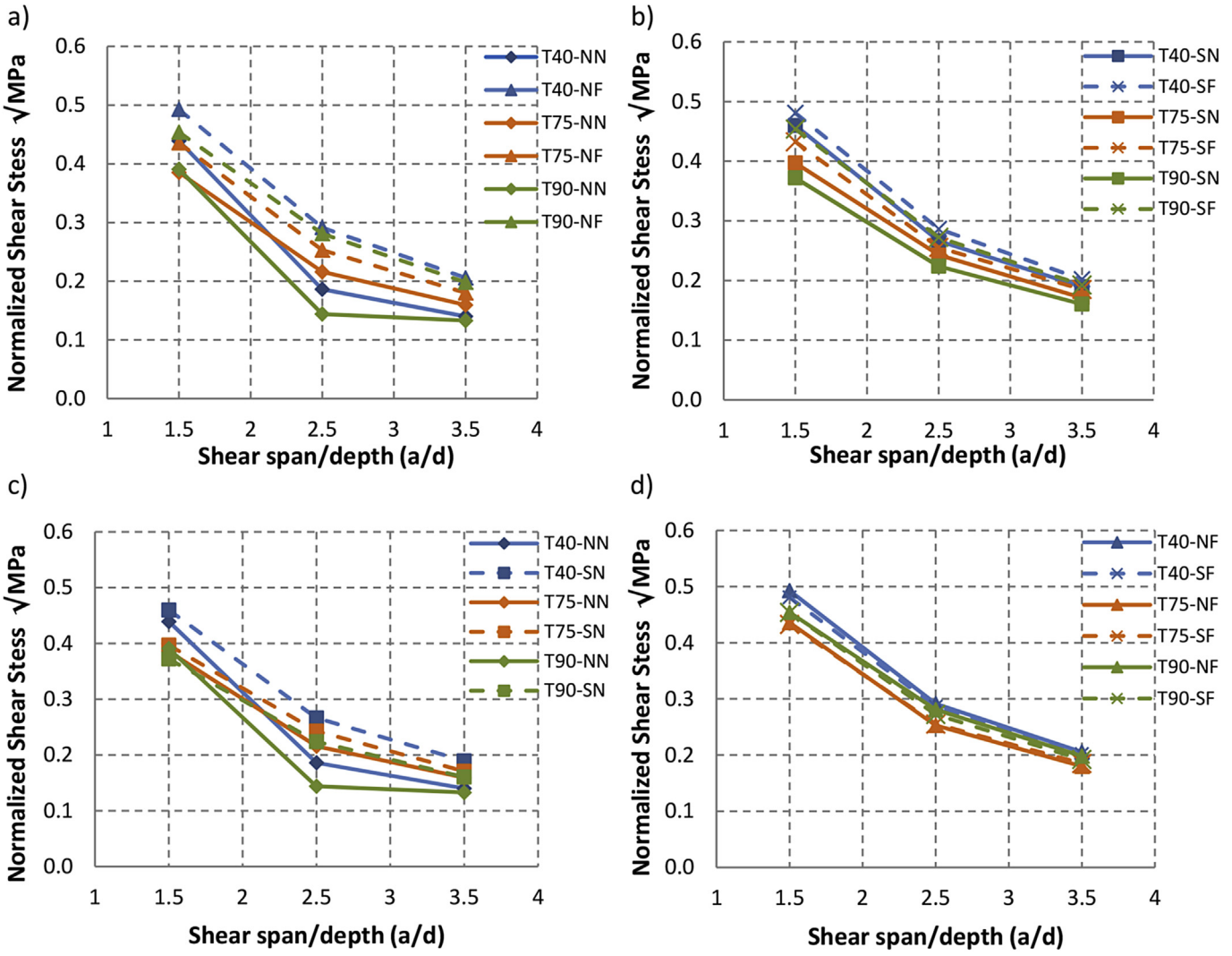

Fig. 8. Normalized shear strength – Beams without (left) and with (right) shear reinforcement.

Fig. 9. Failure of beam T75L-NN: fracture of aggregates.

$$w_{th} = 2l_{s,\max}(\varepsilon_{sm} - \varepsilon_{cm} - \varepsilon_{cs}), \tag{3}$$

where $l_{s,max}$ is the length over which the slip between concrete and steel occurs.

Thus, the maximum crack spacing results $s = 2l_{s,max}$, ε_{sm} and ε_{cm} are the average strains in reinforcement and concrete and ε_{cs} is the strain of the concrete due to free shrinkage.

The length $l_{s,max}$ was evaluated as:

$$l_{s,\max} = k \cdot c + \frac{1}{4}\frac{(f_{ctm} - f_{Ftsm})}{\tau_{bms}} \cdot \frac{\varphi_s}{\rho_{s,ef}}, \tag{4}$$

where k is an empirical parameter that takes into account the influence of the concrete cover (assumed equal to 1), c is the concrete cover, and τ_{bms} is the mean bond strength between steel and concrete assumed to be:

$$\tau_{bms} = 1.8\, f_{ctm},\ \rho_{p,eff} = \frac{A_s}{A_{c,eff}};\ A_{c,eff} = b h_{c,eff} \text{ with } h_{c,eff}$$
$$= \min\left(2.5(h - d);\ \frac{h - x}{3}\ ;\ \frac{h}{2}\right)$$

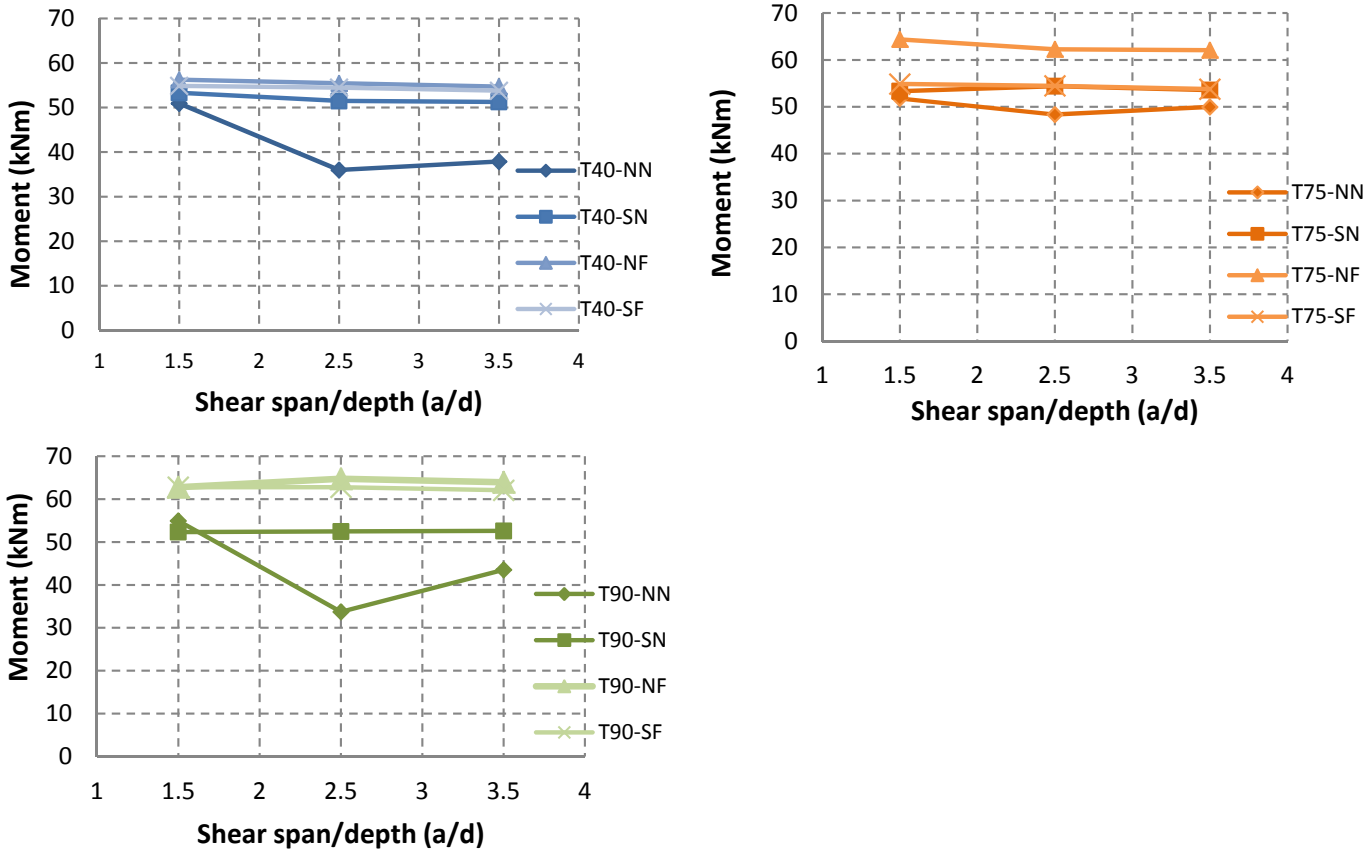

Fig. 10. Ultimate moment as a function of the shear span-to-depth ratio, Concrete T40,75,90.

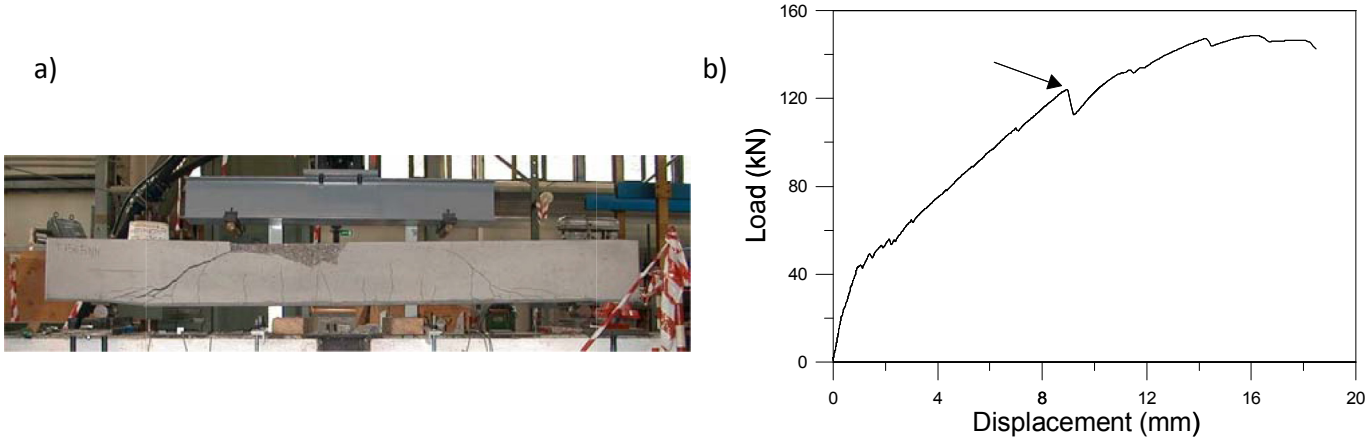

Fig. 11. (a) Failure of beam T75M-NN and (b) load-displacement curve.

The term f_{ctm} is the average value of the tensile strength of the concrete matrix, while the term f_{Ftsm} is considered only for fiber-reinforced concrete; it is a reduced tensile strength according to the procedure described in MC2010 [17].

In particular, $f_{Ftsm} = 0.45 f_{R1}$, where f_{R1} is the tensile strength associated with a CMOD of 0.5 mm experimentally evaluated by three point bending tests according to EN14651 [21] (Table 1, Fig. 1).

The relative mean strain was evaluated as:

$$\varepsilon_{sm} - \varepsilon_{cm} - \varepsilon_{cs} = \frac{\sigma_s - \beta\sigma_{sr}}{E_s} \tag{5}$$

where:

$\beta = 0.6$ (short term loading), σ_s is the steel stress in a crack, σ_{sr} is the maximum steel stress at a crack formation phase:

$$\sigma_{sr} = \frac{f_{ctm} - f_{Ftsm}}{\rho_{s,ef}}\left(1 + \alpha_e \rho_{s,ef}\right) \tag{6}$$

and α_e is the ratio E_s/E_{cm}.

On the basis of the experimental values for the materials' strength, it seems that the cracking behavior of fiber-reinforced

Table 4
Experimental and theoretical, moment at first crack ($M_{cr,\,exp}$, $M_{cr,\,th}$), crack width (w_{exp}, w_{th}) and crack spacing (s_{exp}, s_{th}).

		$M_{cr,\,exp}$ (kNm)	$M_{cr,\,th}$ (kNm)	w_{exp} (mm)	w_{th} (mm)	s_{exp} (mm)	s_{th} (mm)
N	T40	12.22	12.31	0.336	0.327	148.5	221.4
	T75	13.89	13.83	0.359	0.320	162.2	226.4
	T90	12.04	14.31	0.380	0.317	148.6	227.6
	T40F	11.91	12.01	0.265	0.149	93.1	77.7
	T75F	15.33	14.83	0.228	0.145	139.6	75.5
	T90F	15.10	14.13	0.208	0.163	151.7	86.4
S	T40	10.51	12.21	0.298	0.327	168.4	221.4
	T75	12.51	13.72	0.282	0.320	148.6	226.4
	T90	11.75	14.20	0.260	0.317	142.4	227.6
	T40F	12.92	11.92	0.264	0.149	112.5	77.7
	T75F	15.462	14.72	0.244	0.145	94.8	75.5
	T90F	14.421	14.02	0.215	0.163	125.2	86.4

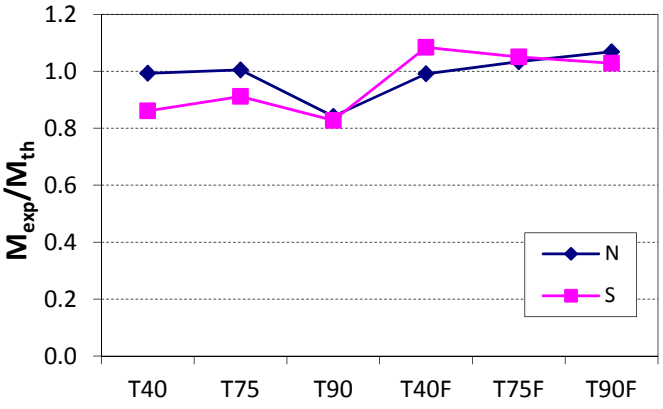

Fig. 12. Ratio between experimental cracking moment and theoretical one.

concrete is not well predicted by MC2010 [17]. The crack width of plain concrete is well estimated particularly in beams without fibers, as shown in Fig. 13 where the ratio between the experimental crack width and MC2010 [17] prediction is plotted. It emerges that the prediction of crack spacing (Table 4) is not accurate for both plain and SFRC. Nevertheless, the crack spacing, evaluated according to MC2010 [17], is the maximum crack spacing; thus, considering an average crack spacing (1.5 $l_{s,max}$), the prediction for plain concrete improves, as shown in Fig. 14, where the ratio between the experimental crack spacing and the average theoretical spacing is plotted.

Regardless, it seems that MC2010 [17] does not well predict the cracking behavior of fiber-reinforced beams. In fact, the crack spacing, and consequently the crack width, depends on an empirical value (k) and several mechanical parameters (Eq. (4)), including the average tensile strength of the concrete matrix f_{ctm} and the reduced tensile strength f_{Ftsm}. The latter is derived from experimental standard tests (three point-bending tests), while the value of the tensile strength f_{ctm} in this study was evaluated by means of splitting tests. Nevertheless, the experimental evaluation of the tensile strength is challenging, as the test methods (direct or indirect) and the boundary conditions in direct tensile tests (freely hinges or fixed platens) [23–26] strongly affect the results. Eq. (4) is highly sensitive even to a slight variation of f_{ctm}; indeed, as shown in Fig. 15, an increase of 10% or 20% in the tensile strength improves the crack width and crack spacing prediction. Similarly, by increasing the empirical value k (suggested equal to 1), better results are obtained. In conclusion, it seems that Eq. (4) still requires some adjustment for fiber-reinforced materials, and further research is needed to better predict the experimental behavior.

4.5. Shear strength

Shear strength is affected by several parameters that are connected even to the concrete composition. For this reason, in the last several decades, many attempts have been made to study the shear strength in special concretes such as high performance, fiber-reinforced, and self-compacting concretes [1,2,5–16,27,28].

Regarding fiber-reinforced concrete, several studies and guidelines propose different equations [7] that consider the fiber effect either within the concrete contribution (accounted using fiber reinforced material properties in tension) or separate from it (accounted with a separate fiber-factor).

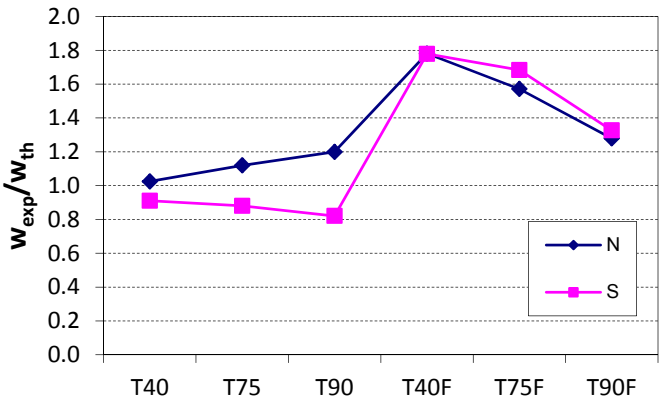

Fig. 13. Ratio between experimental crack width and theoretical one.

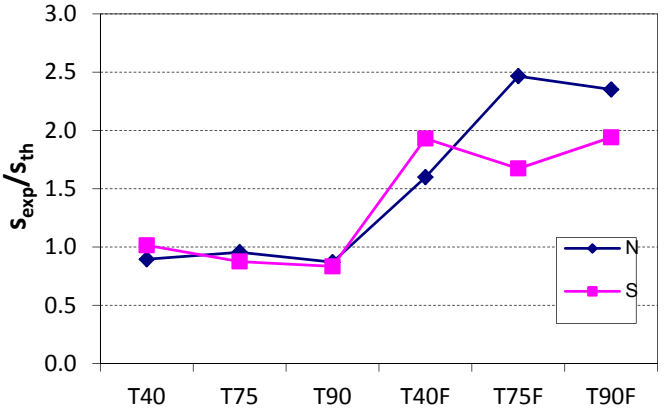

Fig. 14. Ratio between experimental crack spacing and theoretical average value.

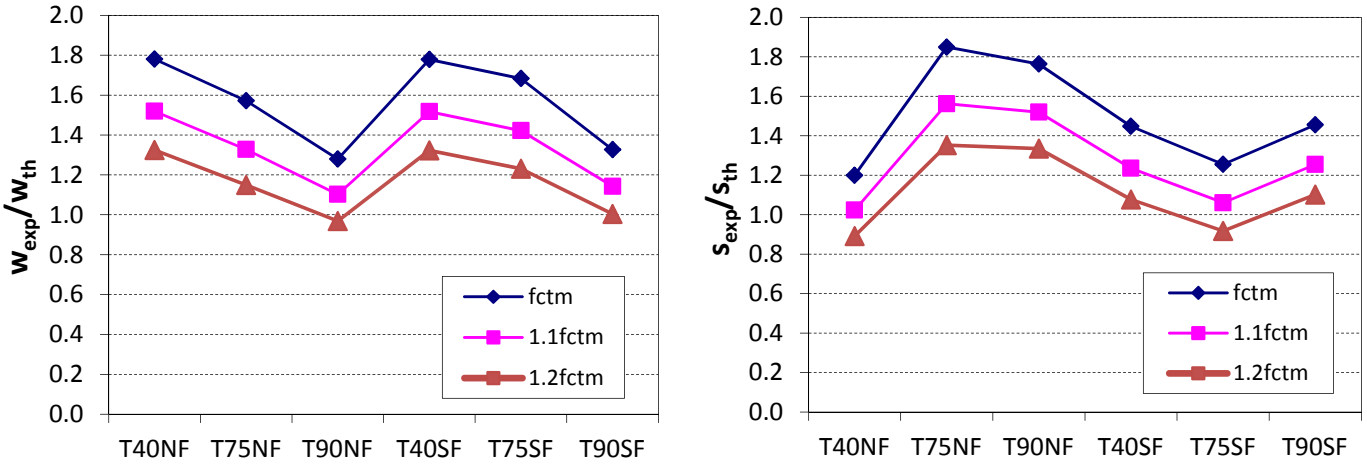

Fig. 15. Fiber reinforced beams: Ratio between experimental crack width/spacing and theoretical one.

Among them, MC2010 [17] proposes a revised formula from EC2 [19] including fiber effect for beams without shear reinforcement:

$$V_{Rd,c} = \frac{0.18}{\gamma_c}\left(1+\sqrt{\frac{200}{d}}\right)\left(100\rho_w\left(1+7.5\frac{f_{Ftuk}}{f_{ctk}}\right)f_{ck}\right)^{1/3}bd \le \left(0.035\left(1+\sqrt{\frac{200}{d}}\right)^{3/2}\sqrt{f_c}\right)bd \tag{7}$$

where γ_c is the partial safety factor (equal to 1.5), while f_{Ftuk} is the characteristic value of the ultimate residual strength at the ultimate crack opening equal to 1.5 mm, and f_{ctk} is the characteristic value of tensile strength of concrete without fibers.

In fact, MC2010 [17] presents a new approach in which the designed shear resistance of a member without shear reinforcement is evaluated at different levels of approximation, also considering the aggregate size and the longitudinal strain at the mid-depth of the effective shear depth (ε_x).

In particular, for a plain concrete member without shear reinforcement, the shear resistance is given by:

$$V_{Rd,c} = k_v\frac{\sqrt{f_{ck}}}{\gamma_c}zb \tag{8a}$$

while for fiber-reinforced concrete, Eq. (8a) becomes:

$$V_{Rd,F} = \frac{1}{\gamma_F}\left(k_v\sqrt{f_{ck}} + 0.8f_{Ftuk}\cot\theta\right)zb \tag{8b}$$

The value $\sqrt{f_{ck}}$ shall not be greater than 8 MPa, while the parameter k_v is defined at different levels of approximation:

$$\text{I level}: \ (f_{ck} \le 70\text{MPa}): \ k_v = \frac{180}{1000+1.25z} \tag{8c}$$

$$\text{II level}: \ k_v = \frac{0.4}{1+1500\varepsilon_x}\cdot\frac{1300}{1000+k_{dg}z} \tag{8d}$$

The parameter that considers the maximum aggregate size d_g is defined as $k_{dg} = \frac{32}{16+d_g} \ge 0.75$.

For concrete strengths higher than 70 MPa, d_g shall be taken as zero to account for the loss of aggregate interlock in the cracks due to fracture of aggregate particles.

k_v is assumed as Eq. (8c) for $\rho_w < 0.08\sqrt{f_{ck}/f_{yk}}$ and as Eq. (8d) for $\rho_w \ge 0.08\sqrt{f_{ck}/f_{yk}}$.

θ is the angle of the compressive stress field relative to the longitudinal axis of the member and

$$29^\circ + 7000\varepsilon_x \le \vartheta \le 45^\circ, \text{ where } \varepsilon_x = \frac{1}{2E_sA_s}\cdot\left(\frac{M_{Ed}}{z}+V_{Ed}\right)$$

A suggested value of ε_x is 0.001, in good agreement with the data from this experimental research.

In the case of beams with shear reinforcement, the shear resistance is given by the concrete ($V_{Rd,c}$) and steel ($V_{Rd,s}$) components:

$$V_{Rd} = V_{Rd,c} + V_{Rd,s} \le V_{Rd,\max} = k_\varepsilon\left(\frac{30}{f_{ck}}\right)^{1/3}\frac{f_{ck}}{\gamma_c}bz\sin\vartheta\cos\vartheta \tag{9}$$

In the case of fiber reinforced concrete, $V_{Rd,c}$ is replaced by $V_{Rd,F}$ (Eq. (8b)), while the steel contribution is defined (with or without fibers) as:

$$V_{Rd,s} = \frac{A_{sw}}{s}zf_{yd}\cot\vartheta. \tag{10}$$

The variable k_ε considers the influence of the state of strain in the web and will be defined depending on the level of approximation:

$$\text{I level}: \ V_{Rd} = V_{Rd,s} \le V_{Rd,\max} \text{ with } \vartheta_{\min} = 30^\circ \quad \text{and} \quad k_\varepsilon = 0.55$$

$$\text{II level}: \ V_{Rd} = V_{Rd,s} \le V_{Rd,\max} \text{ with } \vartheta_{\min} = 20^\circ + 10000\varepsilon_x \text{ and } k_\varepsilon = \frac{1}{1.2+55\varepsilon_1} \le 0.65;$$

$$\varepsilon_1 = \varepsilon_x + (\varepsilon_x + 0.002)\cot 2\vartheta$$

$$\text{III level}: \ V_{Rd} = V_{Rd,c} + V_{Rd,s} \le V_{Rd,\max}(\vartheta = \vartheta_{\min} = 20^\circ + 10000\varepsilon_x)$$

$$k_v = \frac{0.4}{1+1500\varepsilon_x} \cdot \left(1 - \frac{V_{Ed}}{V_{Rd,\max}(\vartheta_{\min})}\right) \geq 0$$

In this research, shear failure was observed only in beams without shear reinforcement and without fibers. Indeed, beams without stirrups but with fibers exhibited the same bending failure as their counterparts with stirrups.

For this reason, the comparison between experimental results and shear code prediction is valuable mainly for beam NN.

A comparison (Table 5) between the experimental observed shear capacity (V_{exp}) and the design resistance evaluated according to MC2010 [17] at the first (Eqs. (8a,8c)) and at second level (Eqs. (8a, 8d)) shows that the code predictions are on the safe side and considerably underestimate the shear strength only for short beams (even accounting for the reduced shear*). It should be highlighted that for beams made with concrete 75 and concrete 90, the shear prediction is the same because of the limit imposed on the value of $\sqrt{f_{ck}} \leq 8$ MPa.

By neglecting that limit and considering the experimental concrete strength and by assuming a safety factor γ_c equal to 1, the ratio between the experimental values and the theoretical ones (Eqs. (8a), (8c) and Eqs. (8a, 8d)) is plotted in Fig. 16.

It seems that even the first level approach is able to predict the experimental behavior, and it is safer than the second level approach. Indeed, the latter seems to be unsafe for medium and long T90 beams (ratio equal to 0.95 and 0.87, respectively) and for long T40 beam (ratio equal to 0.92).

Nevertheless, some inferences can be made even for beams with stirrups and/or fibers.

Table 5
Experimental and predicted shear strength (* Shear strength reduced according to MC2010).

Beam	V_{exp} (kN)	V_{exp} (kN)	V_{Rd} ($\vartheta = 30°$)	
			I level	II level
T40-S-NN	130.51	87.01*	23.05	27.90
T75-S-NN	132.77	88.51*	26.07	31.55
T90-S-NN	140.85	93.90*	26.07	31.55
T40-M-NN		55.31	23.05	27.90
T75-M-NN		74.35	26.07	31.55
T90-M-NN		51.86	26.07	31.55
T40-L-NN		41.62	23.05	27.90
T75-L-NN		54.90	26.07	31.55
T90-L-NN		47.82	26.07	31.55

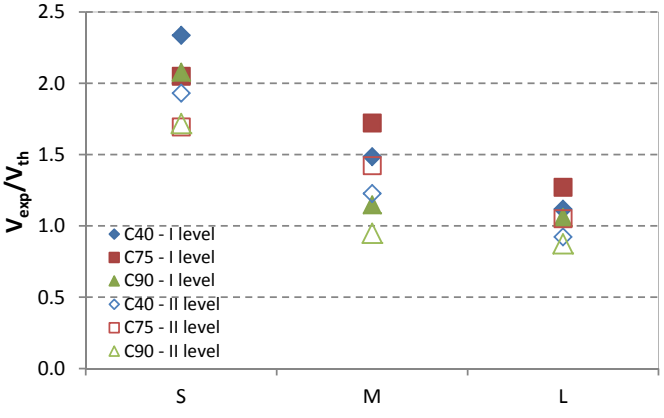

Fig. 16. Beams NN: Ratio between experimental shear strength and theoretical one evaluated at I and at II level.

The MC2010 [17] prediction for beams with stirrups without fibers (SN) is based on the classical approach according to Eq. (10) (first and second level approach). In this case, the ratio between experimental and predicted values varies between 1.32 and 1.53 for short (S) and medium (M) beams, while it lies between 0.94 and 0.98 for long beams; however, since the observed failure was due to flexure, no interesting conclusion can be drawn.

Similar observations can be made for beams with stirrups and fibers (SF), whatever the level approach.

Regarding fiber reinforced beams without stirrups (NF), the shear strength can be evaluated according to Eq. (7) or Eq. (8b). Alternately, among the several prediction methods available in literature [7], an approach is presented that was developed for the fibers considered in this experimental campaign. The latter two predictions give comparable results, while Eq. (7) gives a shear strength of approximately 1/3. Even if we do not know the ultimate shear strength, Eq. (7) is definitely on the safe side. Nevertheless, additional tests with high longitudinal reinforcement ratios to avoid bending failure should be performed to confirm this result.

5. Conclusions

An experimental investigation into the behavior of high performance concrete beams subjected to shear and flexure is presented. The test variables that are adopted as major factors are concrete grade, shear span-to-depth ratio, and the incorporation of web reinforcement (stirrups and/or steel fibers). From the study, the following conclusions may be drawn:

The inclusion of steel fibers in high performance concrete beams causes an important increase in shear and bending strength. For the tested beams, steel fibers may be an alternative to shear reinforcement (1% of volume).

The behavior of all beams up to cracking was similar, after which point beams with fibers (both with and without stirrups) showed not only enhanced strength but also enhanced ductility and stiffness.

Beams with shear reinforcement and/or fibers failed due to the crushing of the compressive zone in a ductile manner, showing the yielding of the longitudinal reinforcement. In beams with fibers, one main crack was usually localized in the central part of the beam.

The normalized shear strength of high strength concrete is lower with respect to normal strength concrete; this drawback is mitigated in fiber-reinforced materials.

For the considered type and amount of fibers, fibers appear to be more effective than stirrups.

The prediction of the design moment and experimental cracking moment based on MC2010 [17] seems to be accurate. Nevertheless, the crack width and the crack spacing prediction are reasonable for plain concrete but unreliable for fiber-reinforced concrete. It appears that code provisions are too sensitive to some parameters (i.e., tensile strength), whereas a calibration of coefficients used in numerical predictions is required.

MC2010 [17] provisions are too conservative for short beams; nevertheless it seems that whatever the level considered, it is able to predict the behavior of high strength SFRC beams.

References

[1] R.N. Swamy, H.M. Bahia, The effectiveness of steel fibers as shear reinforcement, Concr. Int. 7 (3) (1985) 35–40.
[2] Y.K. Kwak, M.O. Eberhard, W.S. Kim, J. Kim, Shear strength of steel fiber-reinforced concrete beams without stirrups, ACI Struct. J. 99 (4) (2002) 530–538.
[3] L. Biolzi, G.L. Guerrini, G. Rosati, Overall structural behavior of high strength concrete specimens, Constr. Build. Mater. 11 (1) (1997) 57–63.

[4] F. Bencardino, L. Rizzuti, G. Spadea, R.N. Swamy, Experimental evaluation of fiber reinforced concrete fracture properties, Compos. Part B Eng. 41 (1)(2010) 17–24.
[5] S. Furlan, J.B. De Hanai, Shear behaviour of fiber reinforced concrete beams, Cem. Concr. Compos. 19 (1997) 359–366.
[6] A.K. Sharma, Shear strength of steel fiber reinforced concrete beams, ACI J. 83 (4) (July-Aug. 1986) 624–628.
[7] H. Aoude, M. Belghiti, W.D. Cook, D. Mitchell, Response of steel fiber-reinforced concrete beams with and without stirrups, ACI Struct. J. 109 (3)(2012) 359–367.
[8] H.H. Dinh, G.J. Parra-Montesinos, J.K. Wight, Shear strength of steel fiber reinforced concrete beams without stirrup reinforcement, ACI Struct. J. 107 (5) (2010) 597–606.
[9] S.A. Al-Ta'an, J.R. Al-Feel, Evaluation of shear strength of fibre-reinforced concrete beams, Cem. Concr. Compos. 12 (2) (1990) 87–94.
[10] H.H. Dinh, G.J. Parra-Montesinos, J.K. Wight, Shear strength model for steel fiber reinforced concrete beams without stirrup reinforcement, J. Struct. Eng. ASCE 137 (10) (2011) 1039–1051.
[11] C. Cucchiara, L. La Mendola, M. Papia, Effectiveness of stirrups and steel fibers as shear reinforcement, Cem. Concr. Compos. 26 (7) (2004) 777–786.
[12] G.J. Parra-Montesinos, Shear strength of beams with deformed steel fibers, Concr. Int. 28 (11) (2006) 57–66.
[13] L. Biolzi, S. Cattaneo, G. Guerrini, Fracture of plain and fiber reinforced high strength mortars slabs with AE and ESPI monitoring, Appl. Compos. Mater. 7 (1) (2000) 1–12.
[14] M. Khuntia, B. Stojadinovic, S. Goel, Shear strength of normal and high-strength fiber reinforced concrete beams without stirrups, ACI Struct. J. 96 (2) (1999) 282–290.
[15] S.A. Ashour, G.S. Hasanain, F.F. Wafa, Shear behaviour of high strength fiber reinforced concrete beams, ACI Struct. J. 89 (2) (1992) 176–184.
[16] S.W. Shin, J.G. Oh, S.K. Ghosh, in: J.I. Daniel, S.P. Shah (Eds.), Shear Behavior of Laboratory-sized High Strength Concrete Beams Reinforced with Bars and Steel Fibers, Fiber Reinforced Concrete: Developments and Innovations, SP-142, American Concrete Institute, Farmington Hills, MI, 1994, pp. 181–200.
[17] FIB, fib Model Code for Concrete Structures 2010, Ernst Sohn Pub., October 2013, ISBN 978-3-433-03061-5, 434 pp.
[18] ACI Committee 318, Building Code Requirements for Structural Concrete (ACI 318-11) and Commentary, American Concrete Institute, Farmington Hills, MI, 2011, 509 pp.
[19] Eurocode 2. Design of concrete structures – Part 1-1: General rules and rules for buildings, EN 1992-1-1, 2004,225pp.
[20] K.K. Choi, P. Hung-Gun, J.K. Wight, Shear strength of steel fiber-reinforced concrete beams without web reinforcement, ACI Struct. J. 104 (1) (2007) 12–21.
[21] UNI EN 14651:2007, Test Method for Metallic Fibre Concrete. Measuring the Flexural Tensile Strength (Limit of Proportionality (LOP), Residual), 2007, 17pp.
[22] G.N.J. Kani, Riddle of shear failure and its solution, ACI J. 61 (4) (1964) 441–467.
[23] S. Cattaneo, G. Rosati, Effect of different boundary conditions in direct tensile tests: experimental Results, Mag. Concr. Res. 51 (5) (1999) 365–374.
[24] S. Cattaneo, G. Rosati, N. Banthia, A simple model to explain the effect of different boundary conditions in direct tensile tests, Constr. Build. Mater. 23 (1) (2009) 129–137.
[25] S. Cattaneo, L. Biolzi, Assessment of thermal damage in hybrid fiber reinforced concrete. Journal of materials in civil engineering, ASCE 22 (9) (2010) 836–845.
[26] A. Vervuurt, J.G.M. Schlagen E,Van Mier, Tensile cracking in concrete and sandstone: part2-effect of boundary rotation, Mater. Struct. RILEM 29 (1996) 87–96.
[27] S. Cattaneo, F. Giussani, F. Mola, Flexural behavior of reinforced, prestressed and composite self-consolidating concrete beams, Constr. Build. Mater. 36 (2012) 826–837.
[28] S. Cattaneo, F. Mola, Assessing the quality control of self consolidating concrete properties, J. Constr. Eng. Manag. ASCE 138 (2) (2012) 197–205.